Supporting Information

Flow-through Capture and *in Situ* amplification Can Enable Rapid Detection of a Few Single Molecules of Nucleic Acids from Several Milliliters of Solution

Travis S. Schlappi,[1] Stephanie E. McCalla,[1] Nathan G. Schoepp, and Rustem F. Ismagilov*

Division of Chemistry and Chemical Engineering, California Institute of Technology
1200 E. California Blvd.; Pasadena, California 91125, United States of America

[1]These authors contributed equally.
*Correspondence to: rustem.admin@caltech.edu; FAX: (626) 568-8743

Table of Contents

S-I. Flow-through capture simulations

The fraction of nucleic acid molecules captured in a membrane pore compared to the amount flowed through (capture efficiency) is a function of pore geometry, flow parameters, and adsorption kinetics (**Figure S-1**). The concentration of nucleic acids at any position in the pore, *C(r, z)*, was simulated at steady-state using the *Transport of Diluted Species* module of *Comsol Multiphysics (version 4.4)* with the parameters listed in **Table S-1**. To generate the data for **Figure 1b-c**, a parametric sweep was performed with various values of $k_{on}\cdot\gamma$, U, R_p, and δ_m (**Table S-2** and **Table S-3**). Then, the inlet flux ($J_{in} = J|_{z = \delta m}$) and outlet flux ($J_{out} = J|_{z = 0}$) were evaluated and used in Eq. S-1 to calculate capture efficiency.

$$Capture\ \% = 1 - \frac{J_{out}}{J_{in}} \qquad \text{(S-1)}$$

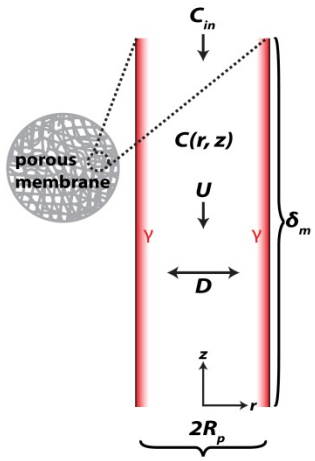

Figure S-1. Schematic of flow-through simulation geometry. Red represents the capture agent (γ) coated on the surface of the pore wall.

Table S-1. Parameters used in the flow-through capture simulations.

Parameter	Description	Value
R_p	Pore radius	0.56 – 17.78 μm
δ_m	Pore length (thickness of membrane)	0.316 – 3162 μm
U	Flow velocity	0.118 – 1000 mm/s
D	Diffusivity of nucleic acid molecule	10 $\mu m^2 \cdot s^{-1}$
k_{on}	Nucleic acid binding rate constant	10^6 $L \cdot mol^{-1} \cdot s^{-1}$
γ	Surface concentration of capture agent	10^{-7} $mol \cdot m^{-2}$
C_{in}	Inlet concentration of nucleic acids	1 μM

Table S-2. The product of $k_{on}\cdot\gamma$ was varied to generate Capture % as a function of Damköhler number (*Da*) (**Figure 1b**). R_p (1 μm), δ_m (100 μm), U (2 mm/s), D (10 $\mu m^2 \cdot s^{-1}$), and C_{in} (1 μM) were held constant.

$k_{on}\cdot\gamma$ (m/s)	k_c (m/s)	*Da*	J_{in} (mol/s)	J_{out} (mol/s)	Capture %
1.00E-07	1.62E-05	0.01	-3.92E-18	-3.88E-18	1.0
2.15E-07	1.62E-05	0.01	-3.92E-18	-3.83E-18	2.1
4.64E-07	1.62E-05	0.03	-3.92E-18	-3.74E-18	4.5
1.00E-06	1.62E-05	0.06	-3.92E-18	-3.55E-18	9.3
2.15E-06	1.62E-05	0.13	-3.92E-18	-3.19E-18	18.5
4.64E-06	1.62E-05	0.29	-3.92E-18	-2.58E-18	34.2
1.00E-05	1.62E-05	0.62	-3.92E-18	-1.75E-18	55.2
2.15E-05	1.62E-05	1.33	-3.92E-18	-9.77E-19	75.0
4.64E-05	1.62E-05	2.87	-3.92E-18	-5.03E-19	87.2
1.00E-04	1.62E-05	6.17	-3.92E-18	-2.94E-19	92.5
2.15E-04	1.62E-05	13.3	-3.92E-18	-2.11E-19	94.6
4.64E-04	1.62E-05	28.7	-3.92E-18	-1.78E-19	95.5
1.00E-03	1.62E-05	61.7	-3.92E-18	-1.63E-19	95.8
2.15E-03	1.62E-05	133	-3.92E-18	-1.57E-19	96.0

Table S-3. U, δ_m, or R_p was varied to generate Capture % as a function of Péclet number (*Pe*) (**Figure 1c**). C_{in} (1 μM), $k_{on}\cdot\gamma$ (10^{-4} m/s), and D (10 $\mu m^2 \cdot s^{-1}$) were held constant.

U (m/s)	δ_m (μm)	R_p (μm)	*Pe*	J_{in} (mol/s)	J_{out} (mol/s)	Capture %
1.18E-04	100	1	0.12	-2.46E-19	-2.32E-36	100.0
2.68E-04	100	1	0.27	-5.32E-19	-1.00E-26	100.0
6.11E-04	100	1	0.61	-1.20E-18	-4.11E-22	100.0
1.39E-03	100	1	1.39	-2.72E-18	-7.21E-20	97.4
3.16E-03	100	1	3.16	-6.19E-18	-1.11E-18	82.0
7.20E-03	100	1	7.20	-1.41E-17	-5.92E-18	58.0
1.64E-02	100	1	16.4	-3.21E-17	-2.02E-17	37.0
3.73E-02	100	1	37.3	-7.30E-17	-5.70E-17	22.0
8.48E-02	100	1	84.8	-1.66E-16	-1.46E-16	12.3
1.93E-01	100	1	193	-3.78E-16	-3.54E-16	6.5
4.39E-01	100	1	439	-8.60E-16	-8.32E-16	3.2
1.00E+00	100	1	1000	-1.96E-15	-1.93E-15	1.6
2.00E-03	3162	1	0.06	-3.90E-18	8.30E-39	100.0

2.00E-03	1000	1	0.20	-3.90E-18	-1.15E-28	100.0
2.00E-03	316	1	0.63	-3.90E-18	-1.72E-21	100.0
2.00E-03	100	1	2.00	-3.90E-18	-2.90E-19	92.6
2.00E-03	31.6	1	6.32	-3.90E-18	-1.50E-18	61.5
2.00E-03	10.0	1	20.0	-3.90E-18	-2.65E-18	32.1
2.00E-03	3.16	1	63.2	-3.90E-18	-3.30E-18	15.4
2.00E-03	1.00	1	200	-3.90E-18	-3.65E-18	6.4
2.00E-03	0.316	1	632	-3.90E-18	-3.80E-18	2.6
2.00E-03	100	0.56	0.63	-1.23E-18	-1.60E-21	99.9
2.00E-03	100	1.00	2.00	-3.90E-18	-2.90E-19	92.6
2.00E-03	100	1.78	6.32	-1.23E-17	-4.20E-18	65.9
2.00E-03	100	3.16	20.0	-3.90E-17	-2.30E-17	41.0
2.00E-03	100	5.62	63.2	-1.23E-16	-9.40E-17	23.6
2.00E-03	100	10.00	200	-3.90E-16	-3.40E-16	12.8
2.00E-03	100	17.78	632	-1.23E-15	-1.15E-15	6.5

Geometry: The model was assembled using a cylindrical geometry drawn in 2D axially symmetric space, with *r* as the radial component and *z* the axial component (Figure S-1). The radius of the cylinder (R_p) varied from 0.56 μm to 17.78 μm; the length of the cylinder (δ_m) varied from 0.316 μm to 3162 μm (**Table S-3**).

Transport: In a porous matrix, fluid flow can be approximated with a uniform velocity (U) independent of radius[1]. The flow velocity varied from $1.18 \cdot 10^{-4}$ m/s to 1 m/s (**Table S-3**). The top boundary of the cylinder ($z = \delta_m$) was an inlet and the bottom boundary ($z = 0$) was an outlet. The diffusion coefficient used was for DNA[2], 10^{-11} m^2/s.

Kinetics: The binding rate between nucleic acids and the capture agent was assumed to be second order with respect to nucleic acid concentration and capture agent surface concentration. We assumed the surface concentration of capture agent (γ) was in excess (and therefore unchanging during the course of the adsorption reaction) and estimated it to be 10^{-7} mol/m^2.

With a kinetic rate constant estimated from nucleic acid-cationic polymer kinetics[3], the adsorption rate occurring at the pore wall is shown in Eq. S-2.

$$R_{ads} = k_{on} \cdot \gamma \cdot C(R_p, z) \tag{S-2}$$

Normally, adsorption kinetics include both an on and off rate. However, in this situation, we excluded the off rate from analysis because it was insignificant compared to the on rate ($k_{on} \sim 10^7$ $M^{-1}s^{-1}$, $k_{off} \sim 10^{-3}$ s^{-1}, reference 38 from the manuscript).

Boundary conditions: The inlet concentration of nucleic acid molecules (C_{in} = 10^{-6} mol/L) represents a normal nucleic acid concentration in human blood plasma[4]. Axial symmetry was imposed at $r = 0$, and a flux boundary condition (Eq. S-3) was imposed at $r = R_p$ to represent the adsorption of nucleic acid molecules to the surface of the pore wall.

$$R_{ads} = D \frac{\partial C(r,z)}{\partial r}\Big|_{r=R_p} \tag{S-3}$$

Mesh and solver settings: The geometry was meshed using a Free Triangular mesh with a maximum element size of 0.0525 μm. The Direct Stationary Solver (PARDISO) was used with a nested dissection multithreaded preordering algorithm and an auto scheduling method.

S-II. Equation 3 and Figure 2b

The number of pores in a membrane (n_p) can be calculated from the porosity (ϕ) as in Eq. S-4.

$$\phi = \frac{n_p \pi R_p^2}{\pi R_m^2} \rightarrow n_p = \frac{\phi R_m^2}{R_p^2} \tag{S-4}$$

The flow rate through the entire membrane (Q) is the flow rate through each pore (Q_p) multiplied by the number of pores ($Q = n_p Q_p$). Using Eq. S-4 for n_p and solving for Q_p gives the following:

$$Q_p = \frac{Q R_p^2}{\phi R_m^2} \tag{S-5}$$

Eq. S-6 results from plugging Eqn S-5 into the relationship between pore flow rate and flow velocity ($Q_p = U\pi R_p^2$).

$$U = \frac{Q_p}{\pi R_p^2} = \frac{Q}{\pi \phi R_m^2} \tag{S-6}$$

Then, using Eq. S-6 in Eq. 2 and setting the condition that $Pe < 1$ yields Eq. S-7.

$$Pe = \frac{U R_p^2}{D \delta_m} = \frac{Q R_p^2}{\pi \phi R_m^2 D \delta_m} < 1 \tag{S-7}$$

Solving Eq. S-7 for Q yields Eq. 3. ϕ = 0.6 and $D = 10^{-11}$ m^2/s were assumed for all calculations.

To calculate the pressure drop as a function of pore radius (R_p) and membrane radius (R_m), Pouiselle flow was assumed (Eq. S-8). Flow rate through the pore (Q_p) was replaced with flow rate through the entire membrane (Q) using Eq. S-5. Q (1 mL/min), μ (10^{-3} Pa·s), and ϕ (0.6) were held constant; R_p and R_m were varied from 1 to 3 μm and 1 to 3 mm, respectively. The results, along with regimes of $Pe < 1$ calculated from Eq. 2, are plotted in **Figure 2b**.

$$\Delta P = \frac{8\mu Q_p \delta_m}{\pi R_p^4} = \frac{8\mu Q \delta_m}{\pi \phi R_p^2 R_m^2} \tag{S-8}$$

S-III. DNA binding efficiency as a function of *Pe*

100 ng of salmon sperm DNA (Invitrogen, CA) in 200 μL of 10 mM MES buffer (pH ~5) was flushed through a chitosan membrane with a radius of 2 mm at different flow rates via the syringe/luer lock system shown in **Figure S-4**. The inlet and eluate DNA concentration of each flush was measured with PicoGreen dye (Invitrogen, CA); converting to mass (m_{DNA}), Eq. S-9 was then used to calculate the capture efficiency.

$$Capture\ \% = \left(1 - \frac{m_{DNA,out}}{m_{DNA,in}}\right) \cdot 100 \tag{S-9}$$

Pe was calculated via Eq. 2 and the results are plotted in **Figure S-2**. This agrees with theoretical predictions that $Pe > 1$ results in reduced capture. Also, layering the nylon membrane with chitosan does not significantly hinder flow rate or require untenable pressure drops to achieve flow rates of ~ 1 mL/min and efficient capture.

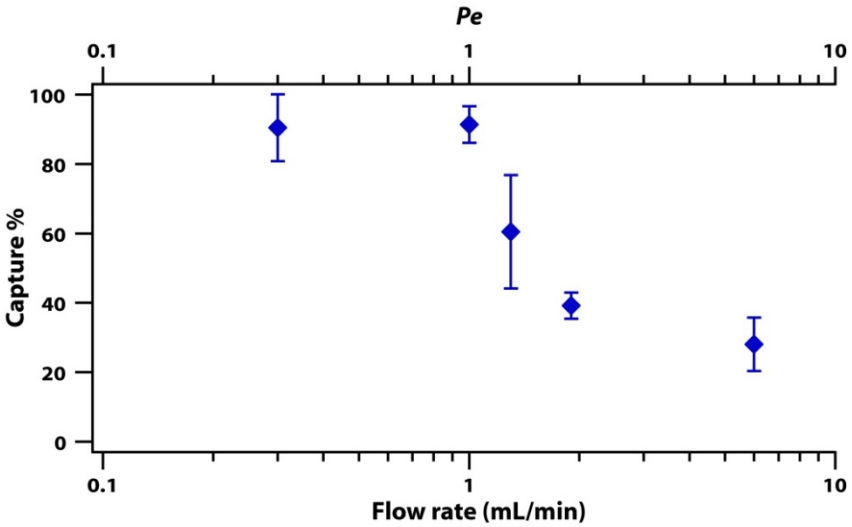

Figure S-2. Capture efficiency depends on flow rate.

We clarify that capture efficiencies > 90% are only possible when the capture agent is in excess of the target DNA molecule and *Pe* < 1, which is the case for 100 ng of input DNA (Figure S-2). On the other hand, the purpose of the experiments in Figure 3 was to measure the total binding capacity of the chitosan membrane (i.e., occupy all the cationic binding sites). To accomplish this, larger quantities of DNA (1000 ng) were flowed through the membrane and the capture efficiency was not expected to be high; in fact, with each successive load, it should decrease to 0% until all binding sites are occupied. Indeed, we observed that the capture efficiency in Figure 3 varied from 60% in the first run to 20% in the fifth run—by the time the fifth load of 1000 ng DNA was flowed through the membrane, there were fewer binding sites available and thus the recovery was much lower than the first load when all binding sites were available.

S-IV. Compatibility of chitosan membrane with *in situ* amplification

To test the compatibility of chitosan membranes with *in situ* PCR amplification, 1 μL of varying concentrations of λ DNA was wetted into chitosan membrane with a radius of 2 mm. The membrane was then placed in a well plate and 10 μL PCR mix was added to the well. Replicates containing 10 μL PCR mix with the same amount of λ DNA and no membrane present were also included. The well plate was inserted into an Ilumina Eco™ real-time PCR System (EC-101-1001) and thermal cycled; correct λ-phage DNA product was verified with melt curve analysis. The PCR mix and thermal cycling conditions used were the same as described in the **Experimental Section**. **Figure S-3a** shows that chitosan membranes are compatible with *in situ* PCR amplification down to ~2 copies/reaction.

To test compatibility with *in situ* LAMP amplification, 20 copies of λ DNA were wetted into a chitosan membrane with a radius of 2 mm. The membrane was then placed in a well plate and 10 μL LAMP mix was added to the well. Replicates containing 10 μL LAMP mix with 20 copies of λ DNA and no membrane present were also included as solution controls. The well plate was inserted into an Ilumina Eco™ real-time PCR System and incubated for 40 min at 68 °C. **Figure S-3b** shows the real-time fluorescent traces representing DNA product.

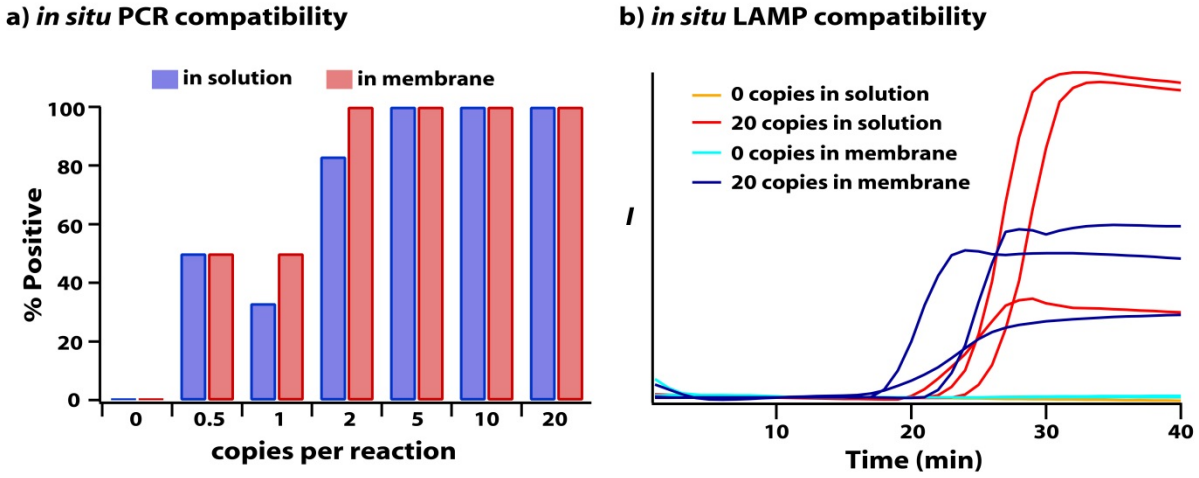

Figure S-3. Compatibility of chitosan membranes with PCR and LAMP amplification. **a)** Dilutions of λ DNA were wetted onto chitosan membranes or placed into a well plate without a membrane; PCR mix was added and amplification was detected via melt curve analysis. Six replicates were run at each dilution; the percent of replicates positive for λ DNA product is shown (n = 6). **b)** 20 copies of λ DNA were wetted onto chitosan membranes within a well plate, or placed into a well plate without a membrane; LAMP mix was added and amplification was detected via real-time fluorescence. Three replicates were run for each sample; the fluorescent traces as a function of time are plotted.

LAMP reagents were purchased from Eiken Chemical (Tokyo, Japan), product code LMP207. The LAMP mixture used for amplification of λ-phage DNA contained the following: 5 µL Reaction Mixture, 0.4 µL of Enyzme Mixture, 0.5 µL of 20X LAMP primer mixture (Table S-6), 0.25 µL of Calcein (Fd), and 3.85 µL of nuclease-free water.

S-V. Details of capture and *in situ* amplification (Figure 5)

Figure S-4 is a schematic of the syringe/luer lock system used to flow mL-scale volumes through chitosan membranes with a radius of 2 mm. Syringes were purchased from BD (Franklin Lakes, NJ) and luer locks (Catalog #LC78-J1A) were purchased from Nordson Medical (Westlake, Ohio). **Table S-4** shows all the quantities of λ DNA, volumes of 10 mM MES buffer, and amounts of background DNA used to generate **Figure 5a**. Salmon sperm DNA from Invitrogen (Carlsbad, CA) was used as "background DNA".

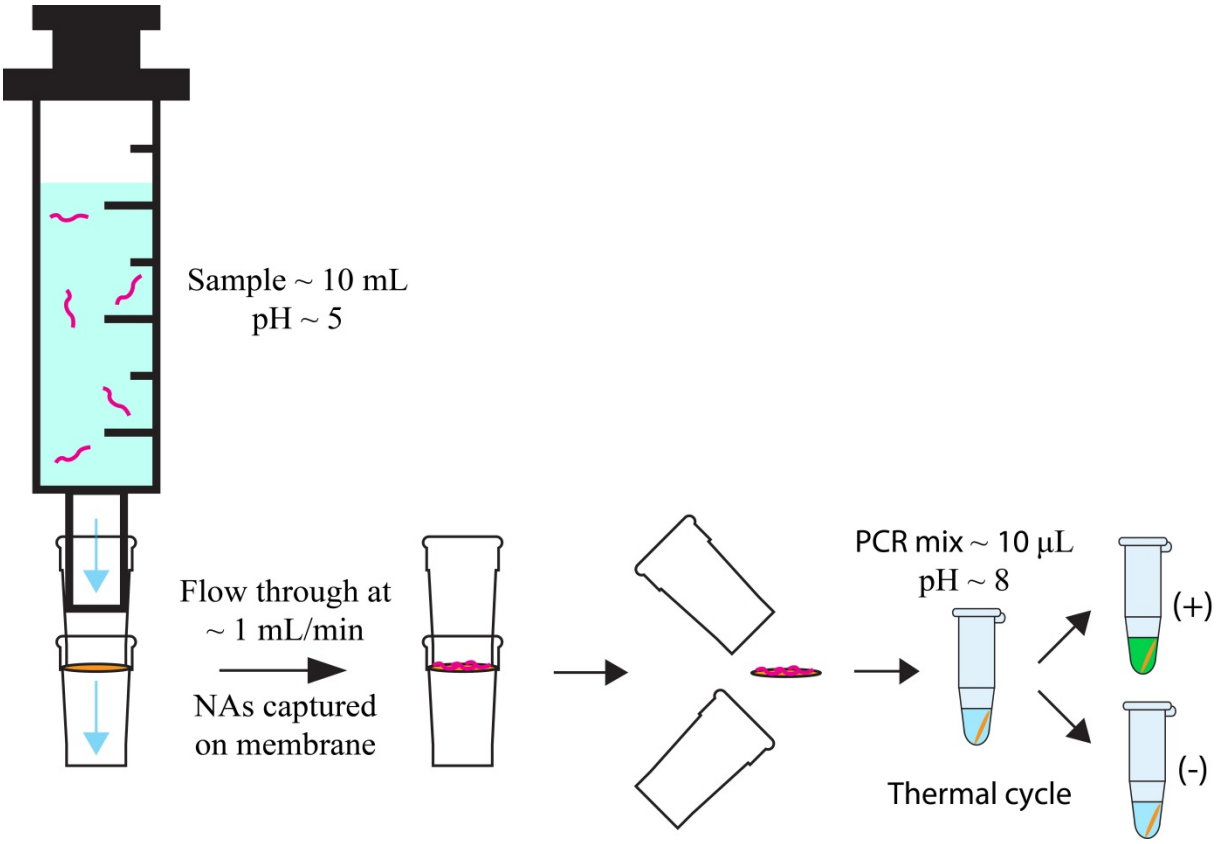

Figure S-4. Schematic of syringe/luer lock system used to flow mL-scale volumes through the chitosan membrane with a radius of 2 mm. A chitosan membrane is placed in between two luer locks. A syringe containing a nucleic acid sample is connected to the top luer lock and the plunger is compressed to flush the sample through the membrane. Then, the luer locks are disconnected from the syringe, taken apart, and the membrane containing captured nucleic acids is placed in a PCR tube along with amplification mix for thermal cycling.

Table S-4. Volumes of 10 mM MES (2-(N-morpholino)ethanesulfonic acid) buffer and final concentrations of λ DNA used for **Figure 5a**. The two fabrication methods are described in the **Experimental Section**.

Copies of λ DNA	Volume of 10 mM MES buffer (mL)	λ DNA Concentration (cop/mL)	Background DNA added to MES buffer (ng)	Positive membranes	Total membranes tested	Fabrication Method
0	1	0	100	0	3	A
0	3	0	100	0	3	B
10	50	0.2	100	1	1	B
10	50	0.2	100	1	4	A
5	15	0.3	100	2	2	A
10	30	0.3	100	1	2	A

10	25	0.4	100	1	2	A
5	10	0.5	100	2	2	A
10	20	0.5	100	3	4	A
25	50	0.5	100	1	1	B
25	50	0.5	0	1	1	B
9	10	0.9	10	6	6	B
5	5	1.0	100	2	2	A
10	10	1.0	100	1	2	A
10	10	1.0	50	3	3	B
9	5	1.8	0	6	6	B
6	3	2.0	100	2	3	B
10	5	2.0	50	2	3	B
12	5	2.4	100	3	3	A
10	4	2.5	100	2	2	A
5	1	5.0	100	5	5	A
10	2	5.0	100	4	4	A
6	1	6.0	100	3	3	B
10	1	10.0	100	3	4	A
20	2	10.0	100	2	2	A
10	1	10.0	0	2	3	B
20	1	20.0	100	5	5	A
20	1	20.0	0	3	3	B

To detect λ DNA product after *in situ* amplification, two methods were used. i) After thermal cycling the membrane with PCR mix in a well plate, an appropriate amount of 6x gel loading dye and TE buffer was added to each well and pipette mixed. Then, 5 μL of this solution was removed from the well, placed in a 1.2% agarose gel, and run for 50 min at 80V. Samples with DNA product at the same length as the λ PCR amplicon (322 base pairs) were considered positive. An example of a gel image is shown in **Figure S-5a**. ii) After thermal cycling, the PCR reaction mixture was transferred to an empty well and an appropriate amount of 20X Evagreen

dye (Biotium) and 10X TE buffer was added. A continuous melt curve was then obtained from 65–95 ˚C; samples with a peak around ~85 ˚C (the melting temperature of the λ PCR amplicon) were considered positive. (**Figure S-5b**).

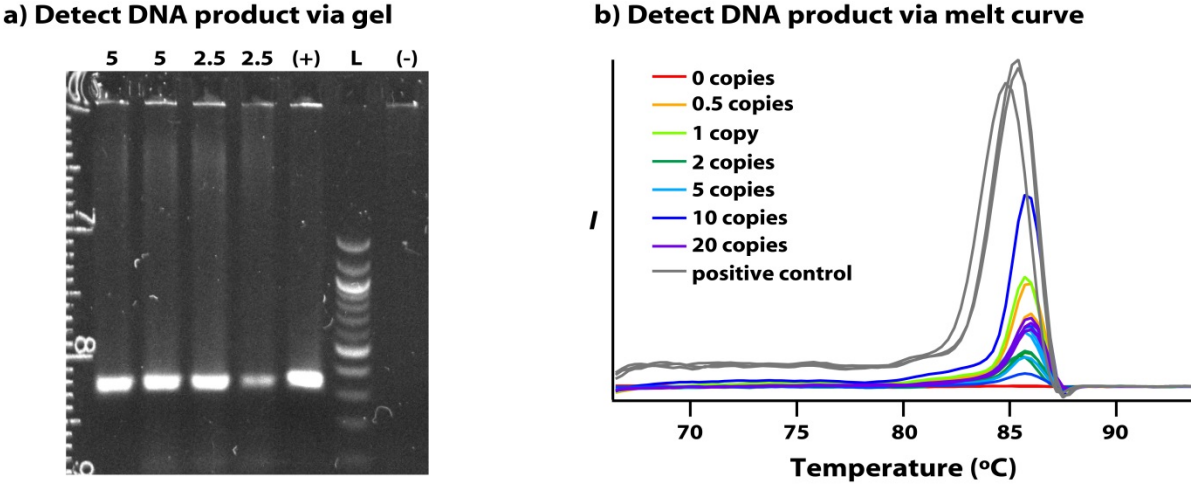

Figure S-5. DNA detection after *in situ* amplification. **a)** Varying concentrations of λ DNA in 10 mM MES buffer were flowed through chitosan membranes. The membranes were then placed in a well plate and thermal cycled. After thermal cycling, each sample was run on a gel. Lanes 1–2: 5 copies/mL; Lanes 3–4: 2.5 copies/mL; Lane 5: positive control (10 copies of λ DNA in PCR mix, no membrane); Lane 6: negative control (0 copies of λ DNA in PCR mix, no membrane). **b)** Dilutions of λ DNA were wetted onto chitosan membranes; PCR mix was added and melt curve fluorescent traces are plotted. Three replicates were run at each dilution.

It is important to note that while **Table S-4** includes experiments done on multiple batches of membranes over 8 months, it does not include all experiments that we performed with chitosan-coated nylon membranes. Using binding capacity measurements (described in **Experimental Section**) and DNA capture experiments (described in **S-V**), we determined that there was batch-to-batch variation in the fabrication process. Therefore, only those batches with consistent performance were analyzed and other batches that did not meet our standards were excluded from analysis.

Table S-5 summarizes **Table S-4** by binning the various experiments into concentration ranges and reporting a "% Positive membranes" along with the standard error. This data is then plotted in **Figure 5a** of the manuscript.

Table S-5. Histogram of **Table S-4** with concentration bins and standard error.

Concentration (cop/mL)	positive	total	positive/total	SE
0	0	6	0.00	0.00
0.2 - 0.5	5	10	0.50	0.16
0.5 - 0.9	6	7	0.86	0.13
0.9 - 2.0	22	25	0.88	0.06
2.0 - 10.0	24	26	0.92	0.05
10.0 - 20.0	8	8	1.00	0.00

To reliably detect ultra-low concentrations of nucleic acids from large volumes, we reduced the background DNA amount to 10 ng and relaxed the constraint imposed on the experiments for **Figure 5a** that the solution be flowed through the membrane at 1 mL/min. We instead flowed through at ~0.3 mL/min and compared 50 mL solutions with 100 ng background DNA to 50 mL solutions with 10 ng background DNA. These experiments showed that 25 copies in 50 mL can be consistently detected when the flow rate and background DNA are reduced from the previous constraints of 1 mL/min and 100 ng. The data is shown in **Table S-6** below and summarized in the manuscript with **Figure 5b**.

Table S-6. Volumes of 10 mM MES (2-(N-morpholino)ethanesulfonic acid) buffer and final concentrations of λ DNA used for **Figure 5b**. The two fabrication methods are described in the **Experimental Section**.

Copies of λ DNA	Volume of 10 mM MES buffer (mL)	λ DNA Concentration (cop/mL)	Background DNA added to MES buffer (ng)	Positive membranes	Total membranes tested	Fabrication Method
25	50	0.5	100	6	10	B
25	50	0.5	10	9	9	B

S-VI. Primer sequences for *λ*-phage DNA PCR amplification and *λ*-phage DNA LAMP amplification

A mixture of primers from **Table S-7** was made at 5 μM each in nuclease-free water and used for the PCR amplification reactions described in this manuscript.

Table S-7. Sequences for λ-phage DNA PCR primers.

forward	CGTTGCAGCAATATCTGGGC
reverse	TATTTTGCATCGAGCGCAGC

A mixture of each primer from **Table S-8** was made in nuclease-free water and used for the LAMP amplification reactions described in **S-IV**. The concentration of each primer in the 20X mixture is also listed.

Table S-8. Sequences for λ-phage DNA LAMP primers[5] and their concentration in the 20X primer mix.

Name	Sequence	Conc.
FOP	GGCTTGGCTCTGCTAACACGTT	4 μM
BOP	GGACGTTTGTAATGTCCGCTCC	4 μM
FIP	CAGCCAGCCGCAGCACGTTCGCTCATAGGAGATATGGTAGAGCCGC	32 μM
BIP	GAGAGAATTTGTACCACCTCCCACCGGGCACATAGCAGTCCTAGGGACAGT	32 μM
LOOPF	CTGCATACGACGTGTCT	8 μM
LOOPR	ACCATCTATGACTGTACGCC	8 μM

S-VII. CDI functionalization of nylon membrane

Before coating with chitosan, the LoProdyne membrane was functionalized with N,N carbonyldiimidazole (CDI) in methylene chloride according to the manufacturer's protocol. The protocol is found at this website (http://www.pall.com/main/oem-materials-and-devices/literature-library-details.page?id=4765) and is also copied below:

> LoProdyne LP membrane has hydroxyl surface chemistry. The membrane binds very little protein in standard binding tests using IgG or BSA. The membrane can be activated for covalent attachment using N, N® carbonyldiimidazole (CDI) in methylene chloride as follows:
>
> 1. Dissolve 0.49 g CDI in 45 mL MeCl2.
> 2. Add to a glass dish under a fume hood.
> 3. Immerse sheet of LoProdyne LP membrane in this solution for 15 minutes, RT.
> 4. Wash membrane 4X with 40 mL per wash MeCl2, 5 minutes per wash.
> 5. Air dry at 60 °C for 3 minutes.
> 6. Store in vacuum desiccator until use.

S-VIII. Complex solutions

To test whether salts in solution could interfere with electrostatic binding and decrease the ability of chitosan membranes to capture and detect nucleic acids, we performed preliminary experiments in complex solutions. Ringer's solution was used to mimic the salt concentration of plasma and was made according to the instructions at the following website: http://cshprotocols.cshlp.org/content/2008/1/pdb.rec11273.full?text_only=true. The information from the website is also pasted below:

Ringer's solution (pH 7.3-7.4)

Reagent (amount to add): NaCl (7.2 gm), CaCl2 (0.17 gm), KCl (0.37 gm).

Dissolve all reagents into reagent-grade H2O, and bring the final volume to 1 L. Adjust the pH to 7.3-7.4. Once thoroughly dissolved, filter through a 0.22-μm filter, aliquot into single-use volumes (25-50 mL), and autoclave.

The final salt concentration of the Ringer's solution is ~125 mM. 5 mM EDTA was also tested because plasma is often processed and stored in an anticoagulant such as EDTA.

S-IX. References

(1) Thömmes, J.; Kula, M. R. *Biotechnol. Prog.* **1995**, *11*, 357-367.
(2) Lukacs, G. L.; Haggie, P.; Seksek, O.; Lechardeur, D.; Freedman, N.; Verkman, A. *J. Biol. Chem.* **2000**, *275*, 1625-1629.
(3) Wink, T.; de Beer, J.; Hennink, W. E.; Bult, A.; van Bennekom, W. P. *Anal. Chem.* **1999**, *71*, 801-805.
(4) Kamm, R. C.; Smith, A. G. *Clin. Chem.* **1972**, *18*, 519-522.
(5) Nagamine, K.; Hase, T.; Notomi, T. *Mol. Cell. Probes* **2002**, *16*, 223-229.

S-X. Author Contributions

Contributions of non-corresponding authors:

Travis S. Schlappi

1. Contributor to method/protocol development for capture experiments and in situ amplification experiments.
2. Major contributor to simulation and theory development.
3. Performed all simulations for Figures 1 and 2.
4. Developed protocol for DNA capacity measurements and performed all experiments for Figure 3.
5. Contributed to experiments and data accumulation for Figure 5.
6. Major contributor to outline, manuscript, and supporting information writing.
7. Major contributor to figure and manuscript revisions.
8. Made all figures and tables in the manuscript and supporting information.

Stephanie E. McCalla

1. Major contributor to concept of chitosan-based flow-through capture and in situ amplification for low concentration detection.
2. Major contributor to method/protocol development for chitosan functionalization (hydrogel and monolayer), capture experiments, and in situ amplification experiments.
3. Major contributor to simulation and theory development.
4. Performed preliminary experimental work on in situ amplification and flow-through capture.
5. Performed preliminary simulations for Figure 1c.
6. Contributed to outline writing.
7. Contributed to manuscript revisions.

Nathan G. Schoepp

1. Major contributor to method/protocol development for chitosan hydrogel synthesis.
2. Contributor to method/protocol development for capture experiments, and in-situ amplification.
3. Contributor to experiments and data accumulation for Figure 5.
4. Minor contributor to manuscript writing.
5. Minor contributor to manuscript revisions.